



OPEN **Glucose influence cold tolerance in the fall armyworm, *Spodoptera frugiperda* via trehalase gene expression**

Anandapadmanaban Gokulanathan¹, Hyoung-ho Mo¹ & Youngjin Park²✉

The fall armyworm (FAW), *Spodoptera frugiperda* is a cold-sensitive species that overwinters in temperate climates without diapause. Overwintering in insects involves rapid cold hardening (RCH), supported by trehalose (TRE), which serves as an intermediate between glycogen (GLY) and glucose (GLU). However, both GLU and TRE help maintain homeostasis under stress. TRE is hydrolyzed by the enzyme trehalase (Treh) into GLU. This study retrieved *Sf-Treh1a*, *Sf-Treh1b*, and *Sf-Treh2* from the FAW transcriptome analysis. RNA interference (RNAi) targeting these three *Treh* genes resulted in significant downregulation of mRNA levels and altered survival rates in RNAi-treated FAW larvae following RCH treatment. High-pressure liquid chromatography (HPLC) quantification of TRE and GLU in treated groups suggests that GLU is an essential component of the hemolymph for survival adaptation to cold conditions in *S. frugiperda*. This study reveals limited cold adaptability of FAW, as evidenced by lower glucose concentration levels. We found that FAW requires alternative molecules, in conjunction with glucose and trehalose for freeze tolerance and survivability. Our study aims to discover the molecular mechanisms that contribute to freeze tolerance in FAW by exploring the roles of trehalose, glucose, and glycogen.

Keywords *Spodoptera frugiperda*, Rapid cold hardening, Trehalase, Overwintering, Transcriptome

The fall armyworm (FAW), *Spodoptera frugiperda* (Smith) (Lepidoptera: Noctuidae), is endemic to tropical and subtropical regions of the American continent¹. Because of its extensive host range as a polyphagous pest, it is ranked as one of the most devastating pests². FAW has spread throughout the Americas, West Africa (Nigeria and Ghana), and Sub-Saharan Africa because of their powerful long-distance migration ability³. Recently, FAW was found in Bangladesh, Myanmar, Thailand, Southeast Asia, and Australia in 2018 and 2019⁴. FAW development is faster at higher temperatures, which helps global spreading, but the FAW's sensitivity to low temperatures and cold conditions significantly limits their worldwide distribution⁵.

Temperature significantly influences the insect's geographic distribution and seasonal activity patterns^{6,7}. Animals that do not hibernate must migrate to survive, as they can only tolerate a narrow range of temperatures during winter^{8,9}. Diapausing insects defend themselves from freezing because of their supercooling ability, known as cold tolerance, which is the most critical aspect of the winter survival of these insects¹⁰. Empirical evidence implies that numerous variables contributing to supercooling and cold hardening abilities are naturally enhanced in insect bodies via cryoprotectants, ice nucleators, and water content^{11,12}. Low weight molecules such as polyols, sugars, antifreeze proteins, and amino acids are well-known cryoprotectants that regulate insects rapid cold hardening (RCH) and supercooling ability¹³. In insects, RCH is a method of cold hardening that occurs in a short time period and helps with survival during sudden cold spells in environments where cold hardiness is lacking¹⁴.

The most frequently used cryoprotectants are sugars, such as trehalose (TRE), glucose (GLU), glycerol, sucrose, and mannitol¹⁵. Glycerol is the most well-studied for cold tolerance, but not TRE and GLU, in insects, including *S. frugiperda*¹⁶ and *Spodoptera exigua*¹⁷. TRE and GLU generally participate in all developmental stages of the insect body, with notable proportions reflecting the combined importance of these two molecules¹⁸. High levels of TRE or GLU are correlated with enhanced RCH in many insects, suggesting their role as cryoprotectants, as evidenced by the higher concentrations of TRE found in the hemolymph of *Anoplophora glabripennis*¹⁹, *Ips typographus*²⁰, and *Chilo suppressalis* larvae compared to other cryoprotectants²¹. Moderately

¹Plant Quarantine Technology Center, Animal and Plant Quarantine Agency, Gimcheon 39660, Korea. ²Department of Plant Medicals, Andong National University, Andong 36729, Korea. ✉email: ypark@anu.ac.kr

increased GLU levels were observed following RCH treatment in the flesh fly *Sarcophaga crassipalpis*²¹ and the Russian wheat aphid *Diuraphis noxia*²². Although the studies mentioned above reported elevated GLU and TRE levels associated with RCH, these increases were specifically linked to the development of cold hardiness²³. GLU and TRE appear to play a role in promoting cold hardiness, thereby enhancing the ability of insects to survive under stress conditions. TRE is well known as the primary circulating sugar in insects; however, glycogen (GLY), a branching polysaccharide of GLU molecules, is the central carbohydrate reserve in the fat body. The onset of energy requires physiological activities metabolizing fat body-stored energy reserves such as GLY and triglycerides²⁴. In sub-zero temperatures, GLY levels went down, and at the same time, TRE increased in *Octadecabacter arcticus*²⁵. A condensation reaction between two GLU molecules, typically sourced from GLY, is required to synthesize the TRE. The TRE is a non-reducing disaccharide composed of two GLU units, synthesized by both trehalose-6-phosphate synthase (TPS) and trehalose-6-phosphate phosphatase (TPP) in most invertebrates, but only in certain insects and crustaceans, it is synthesized exclusively by TPS^{26,27}. Since GLU is essential for TRE anabolism, managing GLU in the fat body directly affects TRE regulation. Trehalase (Treh) is an enzyme that plays a crucial role in the TRE hydrolysis of TRE into GLU and in energy supply. The Treh enzyme is an anomer-inverting glucosidase that catalyzes the hydrolysis of the alpha-glucosidic O-linkage of alpha, alpha- trehalose, releasing initially equimolar amounts of alpha- and beta- D-glucose. Treh is classified as soluble Treh, which hydrolyses intracellular TRE (Treh1), and membrane bound Treh acts both intra- and extracellularly (Treh2) in the beet armyworm, *S. exigua*²⁸.

Several studies have suggested that GLU, Treh1, and Treh 2 are involved in insect metabolism^{29,30}. However, the precise roles of GLU, TRE, and Treh in regulating the cold tolerance in *S. frugiperda* remain unclear. This study investigates the impact of the Treh gene on TRE metabolism relation to cold-hardiness, analysing Sf-Treh1a, Sf-Treh1b, and Sf-Treh2 transcripts, identified in the FAW transcriptome (NCBI accession number: GSE175545). The transcripts were used for RNA interference (RNAi) followed by hemolymph GLU and TRE analysis using HPLC. Additionally, GLY, TRE, and GLU were measured in treated whole larvae using enzymatic assays. This study aims to further elucidate the contributions of Sf-Treh1a, Sf-Treh1b, and Sf-Treh2 to TRE biosynthesis, GLU generation, and GLY conversion, and their roles in cold tolerance mechanisms. The cryoprotectant properties of TRE, potentially mediated through humoral process, may support GLY and GLU mechanism, which are essential for FAW survival during cold periods.

Results

Molecular architecture of trehalose biosynthesis genes

The FAW transcriptome was used to determine full open reading frames (ORFs) of *Sf-Treh1a*, *Sf-Treh1b*, and *Sf-Treh2* of FAW. ORFs of *Sf-Treh1a*, *Sf-Treh1b*, and *Sf-Treh2* encode 579, 588, and 602 amino acid residues, respectively (NCBI accession number: OP359066.1-OP359068.1). Sf-Treh1a, Sf-Treh1b, and Sf-Treh2 proteins contain a single domain structure with the Treh superfamily, as illustrated in Fig. 1A. The phylogenetic analysis indicated that the Sf-Treh1a, Sf-Treh1b, and Sf-Treh2 were clustered with other lepidopteran insects, and the Sf-Treh1b is relatively closer with *Spodoptera litura* and *S. exigua* Treh1. *Manduca sexta*, *Papilio xuthus*, and *Papilio machaon* are clustered with Sf-Treh1a and Treh of *Euphydryas editha*, and *Galleria mellonella* were closer to Sf-Treh2 (Fig. 1B and Table S1). Furthermore, based on comparisons with other well-known insects Treh, all three Treh's three-dimensional structures were predicted using the homology modelling method (Fig. 1C-D). These findings indicated that the sequences of closely matched Sf-Treh1a, Sf-Treh1b, and Sf-Treh2 homologous templates on the server suggest the reliability.

Expression profile of trehalose biosynthesis genes in fall armyworm

In FAW, three trehalase (Treh) genes essential for trehalose biosynthesis (*Sf-Treh1a*, *Sf-Treh1b*, and *Sf-Treh2*) and they ubiquitously expressed across multiple larval tissues, as shown in Fig. 2. During the larval stage, these genes were expressed in various tissues including the head, haemocytes, fat body, midgut, tracheae, central nervous system (CNS), and epidermis as depicted in Fig. 2A, B, and C. The expression of 3 Treh genes was observed in all stages of development, from eggs to adults. However, the expression levels of the Treh genes varied considerably across different tissues and developmental stages. *Sf-Treh1a* expression was significantly different across tissues ($F(6, 14) = 250.45, p < 0.001$), with notably higher expression in haemocytes compared to other tissues, as was observed for *Sf-Treh1b* ($F(6, 14) = 175.32, p < 0.001$). Overall, the ANOVA results indicate moderate biological differences between tissues, with the highest expression levels observed in the haemocytes and tracheae. In contrast, *Sf-Treh1b* displayed the highest expression in the head, fat body, haemocytes, and midgut, which were significantly higher than in the tracheae, CNS, and epidermis ($p < 0.001$). The CNS exhibited the lowest expression levels for both *Sf-Treh1b* and *Sf-Treh2* ($p < 0.05$), showing notable but smaller effects compared to the high expression in haemocytes and head tissues. For *Sf-Treh2*, expression varied significantly across tissues ($F(6, 14) = 290.10, p < 0.001$), with the highest levels in haemocytes, followed by the head and fat body, which also had relatively high expression levels but were significantly lower than in haemocytes ($p < 0.01$). Moderate expression was observed in the tracheae, which was still significantly higher than the CNS ($p < 0.05$). The CNS had the lowest expression of *Sf-Treh2* across all tissues ($p < 0.05$). These results demonstrate significant tissue-specific differences in the expression of Treh genes, suggesting specialized roles for *Sf-Treh1a*, *Sf-Treh1b*, and *Sf-Treh2* in different tissues. Notably, the high expression in haemocytes may indicate their involvement in trehalose metabolism or energy mobilization in immune-related processes, while the expression of *Sf-Treh2* in the head suggests a role in neural or sensory functions. Significant differences in the expression levels of *Sf-Treh1a*, *Sf-Treh1b*, and *Sf-Treh2* were observed across developmental stages (Fig. 2D, E, and F). For *Sf-Treh1a*, one-way ANOVA revealed substantial variation across stages ($F(11, 24) = 450.32, p < 0.001$), with the highest expression observed in adult females (AF), suggesting upregulation associated with adult female physiology. In the case of *Sf-Treh1b*, significant stage-specific differences were also confirmed ($F(11, 24) = 310.21, p < 0.001$).

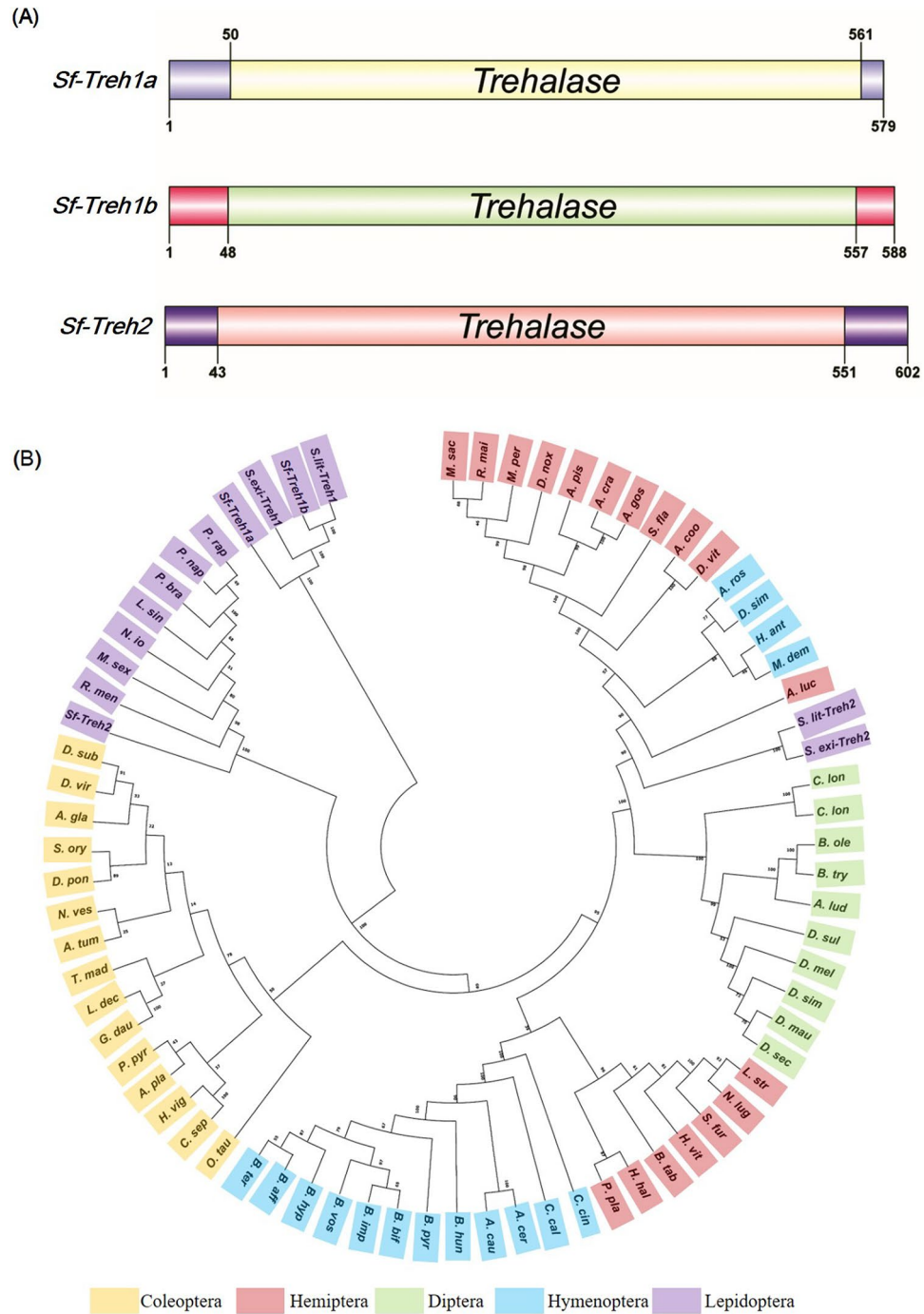


Fig. 1. Protein domain analysis and three-dimensional structures of trehalase genes of *S. frugiperda*. (A) Prediction of signature motifs of trehalase. The functional domains were predicted using the NCBI conserved domain database and the EMBL-EBI HMMER database. (B) Phylogenetic analysis of trehalase genes, including *Sf-Treh1a*, *Sf-Treh1b*, and *Sf-Treh2* of *S. frugiperda* with *S. litura* Treh1 (Sl-Treh1) and Treh2 (Sl-Treh2), *S. exigua* Treh1 (Se-Treh1) and Treh2 (S2-Treh2), and other insects' species from different orders. The analysis was performed using MEGA X. Each node contains a bootstrap value after 1,000 replications to support branching and clustering. (C) Alignment of amino acid sequences of trehalase genes from *S. frugiperda*, *S. litura*, and *S. exigua*. Alignment was performed using Clustal Omega online server and viewed using Jalview 2.11.2. (D) Three-dimensional protein structures of *Sf-Treh1a*, *Sf-Treh1b*, and *Sf-Treh2*, *Sf-Treh1*, *Se-Treh1*, *Sl-Treh2*, and *Se-Treh2*. *Sf-Treh1a*, *Sf-Treh1b*, and *Sf-Treh2* were superimposed with the same protein from *S. litura* and *S. exigua*. All abbreviation and related explanation are shown in Table S2.

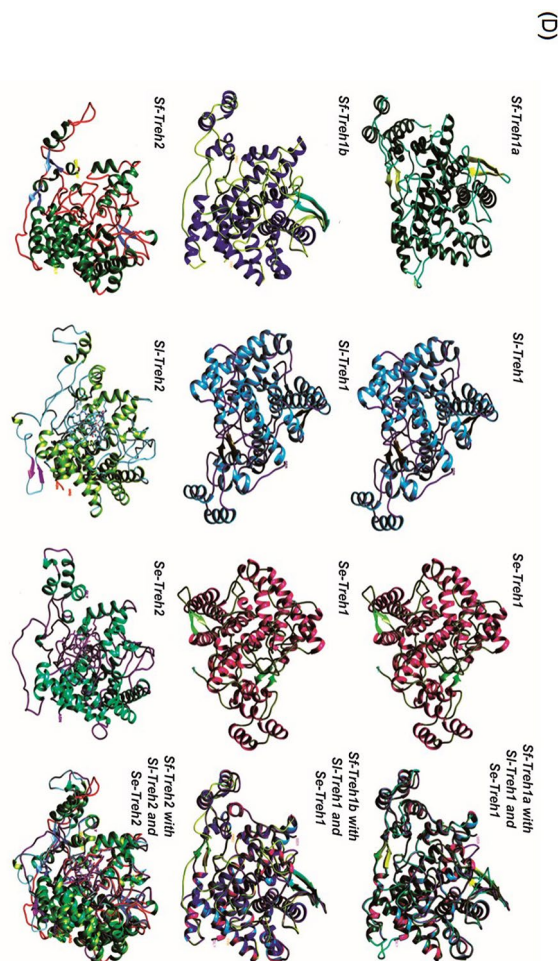


Figure 1. (continued)

RNA interference to *Sf-Treh* genes affect trehalose and glucose concentrations in hemolymph following rapid cold hardening

We conducted an effective RNAi assay to investigate the impact of gene knockdown on the expression of *Sf-Treh1a*, *Sf-Treh1b*, and *Sf-Treh2* in FAW larvae. Three micrograms of dsRNA for each gene were injected into each larva. Our analysis revealed a significant decrease in the mRNA level expression of all three genes at 48 h post-RNAi treatment (Fig. 3A). The reduction in expression was most pronounced for *Sf-Treh1a*, with the knockdown effect evident as early as 24 h and persisting through 48 h (Kruskal-Wallis test, $H(3, 31) = 92.86$, $p < 0.01$). Similarly, *Sf-Treh1b* and *Sf-Treh2* showed notable reductions, though their knockdown effects were less compared to *Sf-Treh1a*. Levene's test for homogeneity of variance produced a near-significant result ($F(3, 64) = 1.63$, $p < 0.01$), suggesting that the variances across groups were marginally different and necessitating careful interpretation of results.

Post-hoc analyses revealed that the most significant reductions occurred between 0 and 48 h for *Sf-Treh1a* ($p < 0.01$), while *Sf-Treh1b* and *Sf-Treh2* exhibited milder but significant decreases. These results highlight the differential sensitivity of the three genes to RNAi-induced suppression. While *Sf-Treh1a* experienced the most intense decline in expression level, both *Sf-Treh1b* and *Sf-Treh2* demonstrated varying levels of resilience, particularly *Sf-Treh2*, which exhibited a more gradual reduction in expression. *Sf-Treh1a* appears to play a critical role in trehalose metabolism, showing the greatest knockdown effect, while *Sf-Treh1b* and *Sf-Treh2* likely contribute to metabolic regulation with varying degrees of RNAi resistance.

A rapid and sensitive HPLC protocol was developed to analyze trehalose (TRE) and glucose (GLU) simultaneously (Fig. 3B). The protocol was validated for accuracy and precision, ensuring the reliability of the results. Each *Sf-Treh* gene-specific dsRNA injection showed a significant increase in TRE levels compared to the control group (dsEGFP) (Kruskal-Wallis test, $H(3) = 18.72$, $p < 0.01$). The ds*Sf-Treh1a* group exhibited the highest trehalose concentration at 11.26 mM, while the ds*Sf-Treh1b* and ds*Sf-Treh2* groups had concentrations of 8.214 mM and 7.95 mM, respectively (Fig. 3C). ANOVA results further confirmed significant differences in trehalose concentrations across treatments: *Sf-Treh1a* ($F(1, 4) = 21.33$, $p < 0.05$), *Sf-Treh1b* ($F(1, 4) = 30.40$, $p < 0.05$), and *Sf-Treh2* ($F(1, 4) = 18.20$, $p < 0.05$). Pairwise comparisons confirmed that *Sf-Treh1a* knockdown had the strongest effect on trehalose levels.

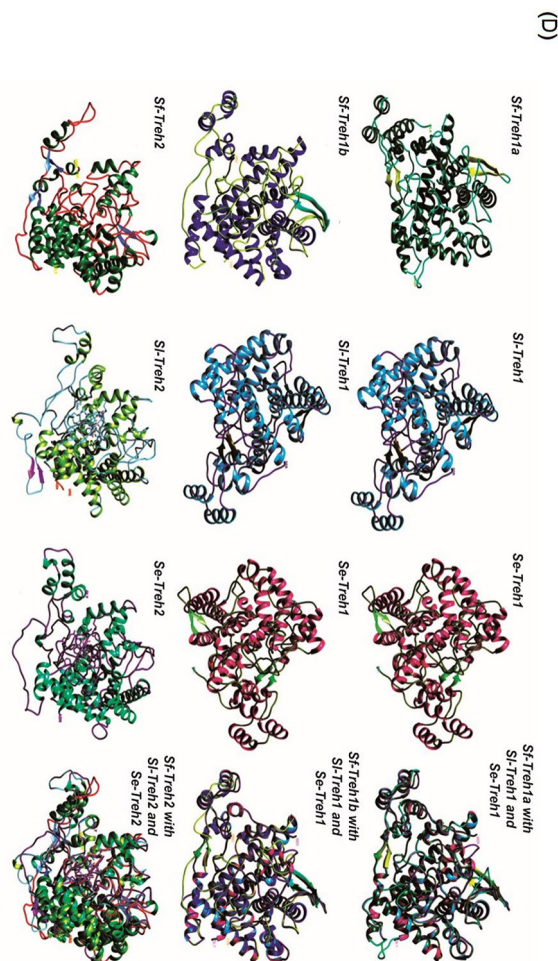


Figure 1. (continued)

Effect of dsTreh's on trehalose, glycogen, and glucose concentrations in whole body following rapid cold hardening

The concentrations of glycogen (GLY), trehalose (TRE), and glucose (GLU) in the whole bodies of FAW larvae were measured and normalized per milligram of protein. We used one-way ANOVA, followed by Tukey's post-hoc test, for statistical analysis. Significant differences in glycogen levels were found, with the dsSf-Treh1a treated group showing much higher glycogen concentrations compared to the control group ($F(5,6) = 31.68$, $p < 0.01$). The dsSf-Treh1b and dsSf-Treh2 groups showed lower glycogen levels than the control, with differences that were still statistically significant ($F(5,6) = 31.68$, $p < 0.01$) (Fig. 4A). Trehalose content was also significantly increased across all treated groups, with the dsSf-Treh1a, dsSf-Treh1b, and dsSf-Treh2 groups showing higher trehalose levels than the dsEGFP control ($F(5,6) = 26.19$, $p < 0.01$), with the largest increase in the dsSf-Treh1a group (Fig. 4B). For glucose, the dsSf-Treh1a group showed a notable reduction in concentration compared to the control ($F(5,6) = 18.24$, $p < 0.01$), and both the dsSf-Treh1b and dsSf-Treh2 groups also had significantly lower glucose levels relative to the control ($F(5,6) = 18.24$, $p < 0.01$) (Fig. 4C).

These findings suggest that RCH modulates glycogen, trehalose, and Treh levels differently depending on the specific Treh gene targeted, with these changes playing a crucial role in cold tolerance.

Survival reductions in cold condition

Following the successful suppression of the three Treh dsRNAs in larvae at 48 h, survival rates were measured. Larvae subjected to rapid cold hardening (RCH) showed a significant decrease in survival rates. A one-way ANOVA was conducted to compare survival rates among the RCH-treated groups injected with dsSf-Treh (dsSf-Treh1a, dsSf-Treh1b, dsSf-Treh2) and the control groups injected with dsEGFP. The ANOVA results indicated a statistically significant overall effect of the treatments on survival ($F(3,8) = 31.94$, $p < 0.001$). Specifically, survival in the dsSf-Treh1a injected group was significantly lower than in the dsEGFP control group ($p < 0.001$). Similarly, significant decreases in survival were observed in the dsSf-Treh1b ($p = 0.002$) and dsSf-Treh2 ($p = 0.004$) groups compared to the control (Fig. 5).

Post-hoc analyses using Tukey's test confirmed that all pairwise comparisons between the dsSf-Treh-treated groups and the control were statistically significant. Assumption checks using Levene's test indicated that the ANOVA assumption of homogeneity of variances was met ($p = 0.184$), validating the robustness of these results.

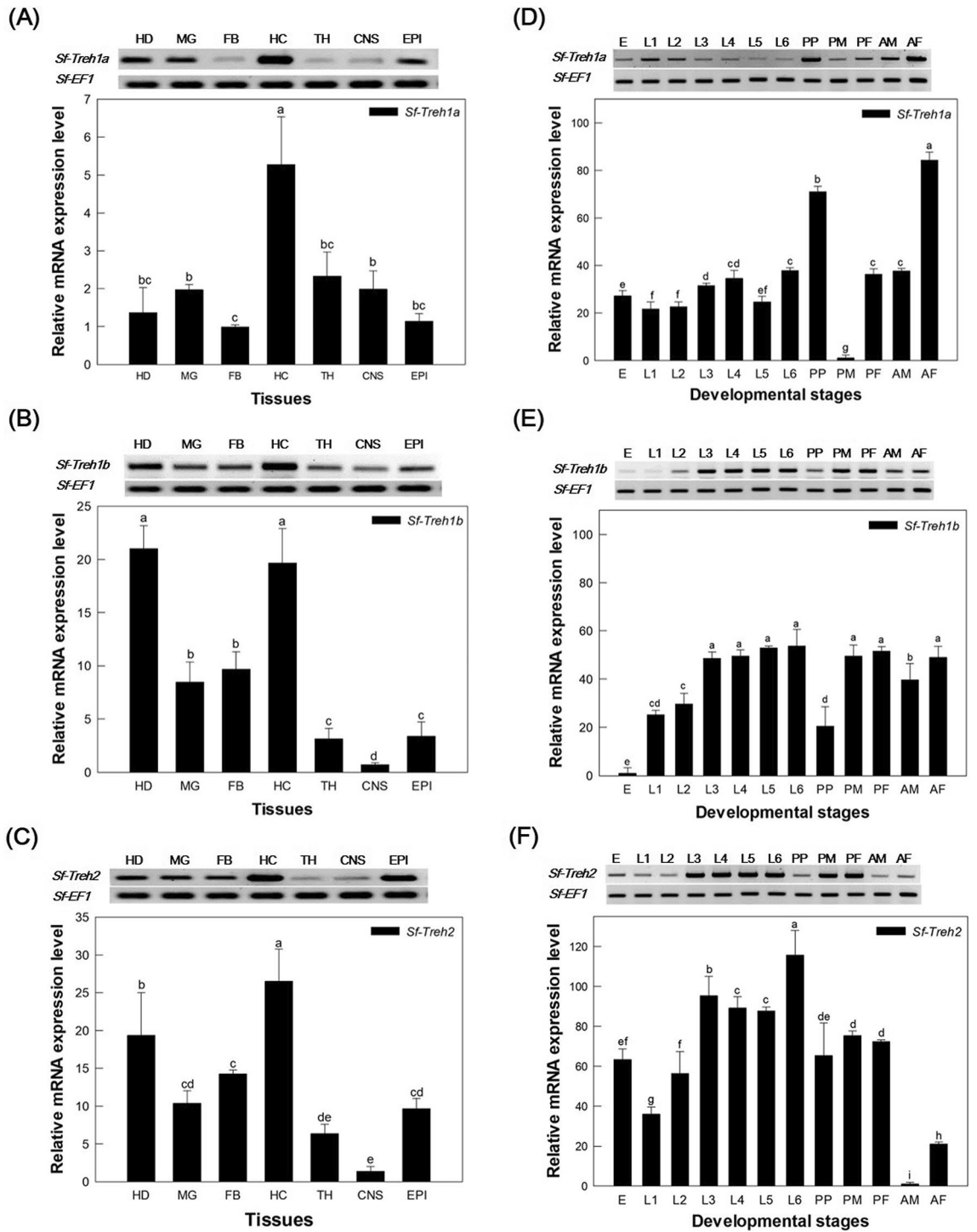


Fig. 2. Expression profile of trehalase genes in *S. frugiperda*. RT-PCR analysis of *Sf-Treh1a*, *Sf-Treh1b*, and *Sf-Treh2* in different tissues (A, B, and C) and developmental stages (D, E, and F). Different tissues include HD: head; MG: midgut; FB: fat body; HC: hemocyte; TR: tracheae; CNS: the central nervous system; ED: the epidermis and different developmental stages include egg (E), larvae instars (L1–L6), pre-pupa (PP), pupa male (PM), pupa female (PF), adult male (AM), and adult female (AF). The *EF1* expression was used to validate complementary DNA integrity for RT-PCR and as an internal control for RT-qPCR. Each experiment was replicated three times. one-way ANOVA followed by post-hoc Tukey’s HSD test was performed for tissue profile. In the developmental stage expression profile, either one-way or two-way ANOVA, followed by Tukey’s HSD for pairwise comparisons, was applied. Different letters above standard deviation bars indicate significant differences.

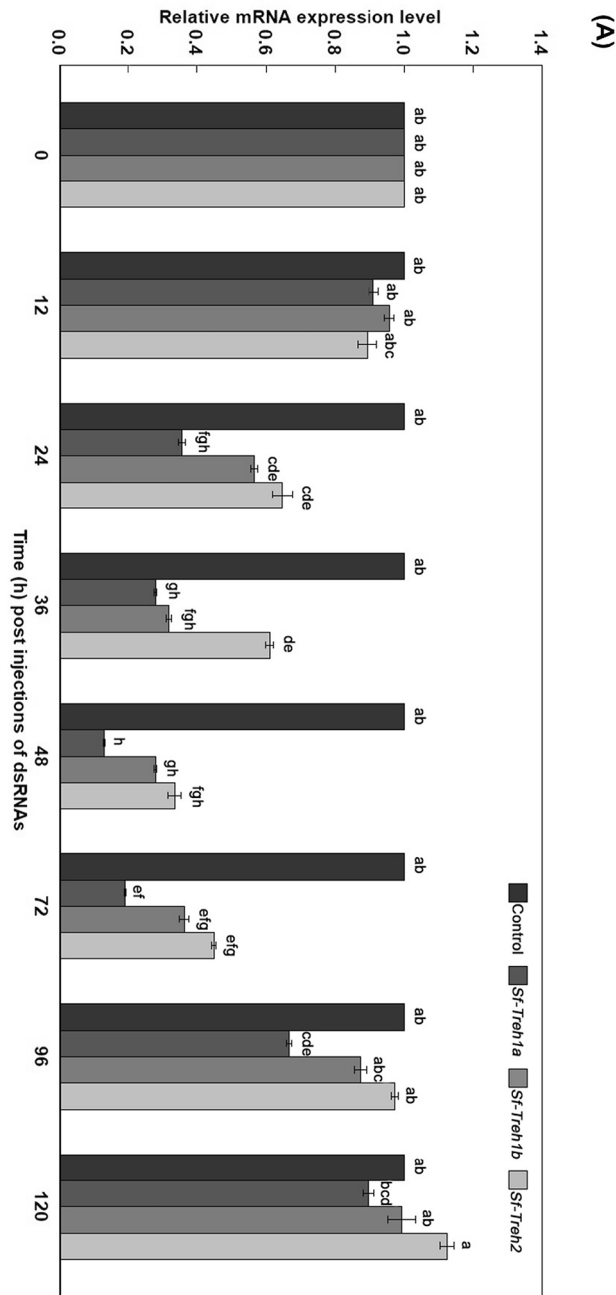


Fig. 3. RNA interference (RNAi) to *Sf-Treh* genes affect trehalose (TRE) and glucose (GLU) concentrations in *S. frugiperda* hemolymph following rapid cold hardening (RCH). **(A)** The effect of RNAi to specific trehalase genes of *S. frugiperda*. All dsRNAs specific to target trehalase genes were constructed at ~300–400 bp and injected into each L5 at 3 μ g. Control RNAi (dsEGFP) was injected with dsRNA specific to the EGFP gene. RT-qPCR shows the changes in mRNA expression levels of *Sf-Treh1a*, *Sf-Treh1b*, and *Sf-Treh2* after RNAi. *EF1* was used to validate cDNA integrity. To assess the effects of dsRNA injections on the mRNA expression patterns of *Sf-Treh1a*, *Sf-Treh1b*, and *Sf-Treh2* across different time points, a series of statistical tests were conducted. First, the normality of the data was evaluated using the Shapiro-Wilk test ($p < 0.05$). Homogeneity of variance across groups was assessed using Levene's test ($p > 0.05$). A Kruskal-Wallis test was used to compare gene expression levels across different time points. Post-hoc pairwise comparisons were performed using Dunn's test with Bonferroni correction. Significant pairwise differences were identified by Dunn's test and are represented by distinct significance letters in the corresponding bar plots. **(B)** Trehalase and glucose chromatogram of HPLC that shows the effect of RNAi specific to trehalase genes (48 h post dsRNAs injection) and RCH treatment in the hemolymph of fifth instar larvae. **(C)** The TRE and GLU concentrations in hemolymph analysed by HPLC. Error bars represent the standard error of the mean (SE). Statistically significant differences between the treatment groups and control (dsEGFP) are indicated by asterisks (* $p < 0.05$, ** $p < 0.01$, *** $p < 0.001$), as determined by one-way ANOVA followed by Tukey's post-hoc test. Replications of all treatments were carried out three times with 10 individuals per replication.

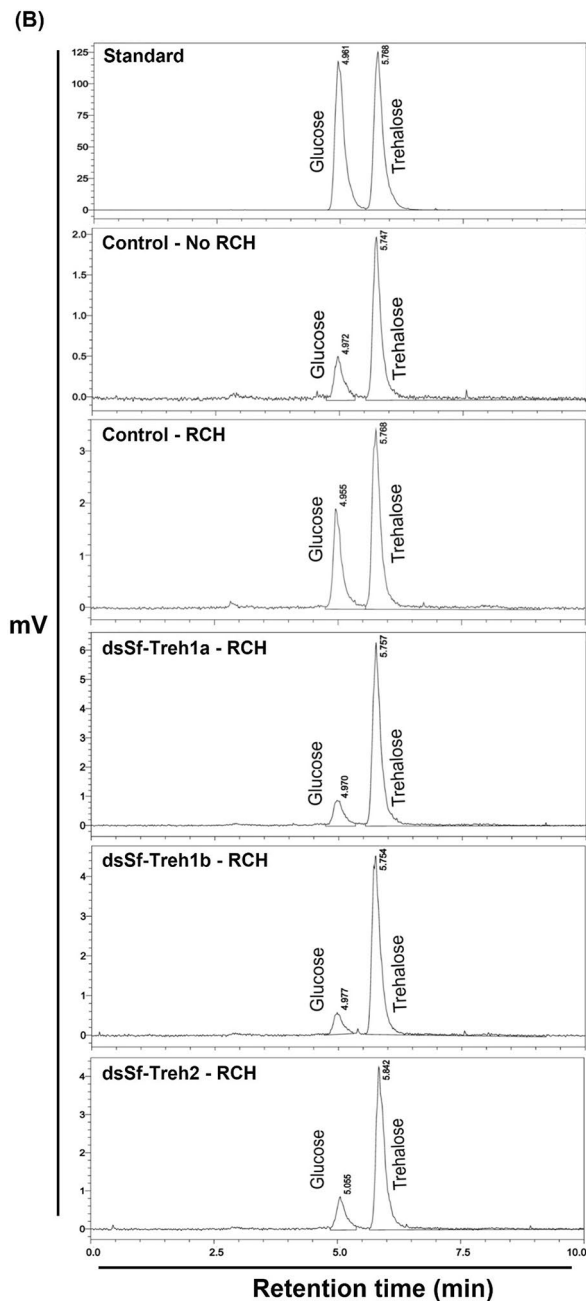


Figure 3. (continued)

These findings strongly suggest that suppression of the Treh genes significantly compromises larval survival under cold conditions, emphasizing the essential role of Treh in helping larvae adapt to environmental stressors like rapid cold hardening.

Discussion

Our findings provide insight into the role of trehalose (TRE), glycogen (GLY), and glucose (GLU) in the cold tolerance mechanisms of *S. frugiperda* larvae, particularly under rapid cold hardening (RCH) conditions. Insects, including *S. frugiperda*, employ mechanisms such as cryoprotectant production, supercooling, and metabolic depression to withstand sudden cold exposure^{31,32}. This study demonstrates that knockdown of TRE-regulating genes *Sf-Treh1a*, *Sf-Treh1b*, and *Sf-Treh2* significantly alters hemolymph levels of TRE and GLU, aligning with the cryoprotective and energy-regulating roles of these sugars during cold stress^{33,34}. TRE's elevation following gene-specific RNAi treatment highlights its protective role against cold-induced cellular damage, consistent with findings from other insect studies that report increased TRE levels to prevent cellular injury at low temperatures³⁵. The observed interplay between TRE, GLY, and GLU suggests that GLY breakdown contributes to TRE and GLU synthesis, providing essential resources to sustain physiological functions critical for cold

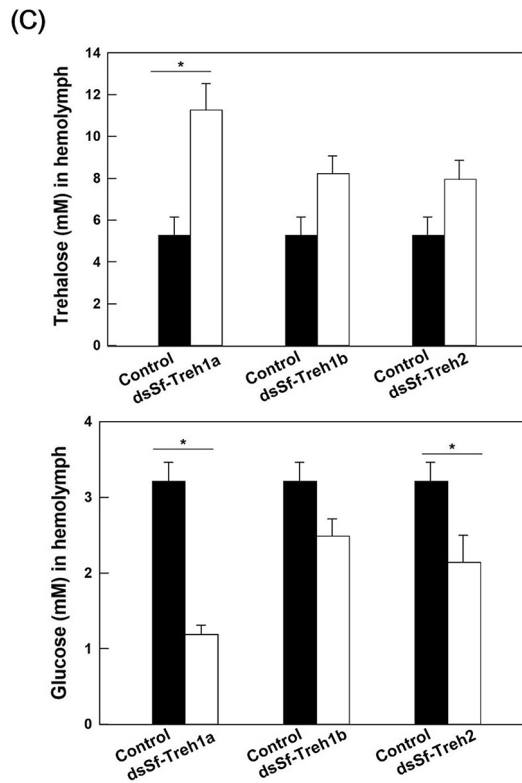


Figure 3. (continued)

survival, such as cryoprotection, energy metabolism, and ion balance across cell membranes³⁶. Additionally, our results support the hypothesis that increased TRE and GLU during RCH enables rapid cold tolerance adaptation, preserving cellular integrity and metabolic function during sudden temperature drops³⁷. Overall, our study advances understanding of how FAW larvae use TRE and GLU synthesis as part of a broader RCH response to enhance cold tolerance. This enhanced metabolic response may offer targets for further investigation into genetic and biochemical pathways involved in insect cold hardiness, with implications for managing FAW populations in colder climates³⁸. This adaptive response can significantly improve cold tolerance, which can occur within minutes or hours of exposure to cold (Fig. 6).

The insect TRE, GLU, and GLY pathways refer to the metabolic processes through which insects utilize and store carbohydrates for energy and survival³⁹. TRE counteracts cold stress in insects by metabolizing GLU via Treh, which can then be utilized in glycolysis to generate ATP⁴⁰. The enzyme Treh has various effects on insect cold tolerance, including the regulation of TRE metabolism⁴¹. For example, the cold temperature-acclimated egg parasitoid wasp *Trichogramma dendrolimi* exhibited increased Treh activity or expression⁴². Five Treh genes have been cloned in *Tribolium castaneum* to study their functions using RNAi⁴³. Therefore, we used RNAi to investigate the effect of RCH on the expression of three Treh genes on TRE, GLU, and GLY synthesis. Both genes were expressed and linked to the TRE biosynthesis pathway, affecting GLU and GLY formation. Therefore, we believe that cold tolerance depends on TRE, but GLU and GLY also play significant roles.

The RNAi pathway is an essential biological process in attempts to suppress insect gene expression. Introducing dsRNA into an insect can cause the breakdown of the intended messenger RNA (mRNA), thereby reducing protein production. The current results show that dsSf-Treh1a, 1b, and 2 can reduce Treh activity, leading to alterations in GLY, TRE, and GLU contents. The dsRNA of Treh affects biochemical metabolism and causes a significant increase in TRE content and a decrease in GLU and Treh activity³⁹. Because the RNAi targeted *Sf-Treh1a*, *1b*, and *2*, the TRE significantly increased in the treated groups, and it was shown that all Treh's catalyzed the hydrolysis of TRE to generate Treh. However, dsSf-Treh1a has a more significant effect than dsSf-Treh1b and dsSf-Treh2 on decreasing *Sf-Treh1a* expression and GLU content and increasing GLY, as evidenced by the current RNAi functional study, TRE has physiological significance in RCH. This indicated that *Treh* knock-down led to a shift in their metabolism toward TRE accumulation and away from GLU production. Similar results showed that dsRNA Treh injection reduced Treh activity, increased TRE levels, and decreased GLY and GLU levels in the fat body⁴³. A previous study revealed that Treh2 protein expression increased significantly, while Treh1 protein was not detected due to the hydrolysis of TRE into GLU for GLY storage. In addition, Treh2 targets TRE hydrolysis into GLU, which enters the oocytes, demonstrating that Treh2 functions in energy metabolism^{44–46}.

Although phenotypic flexibility often has a more significant effect on cold tolerance, there is still a correlation between genetic adaptability and cold resilience in insects. However, rapid cold hardening (RCH) appears to inhibit cold adaptation and diapause without significantly altering gene expression^{47,48}. In the present study, TRE and GLU levels were analyzed by HPLC. FAW larvae treated with dsRNA targeting the specific Treh gene

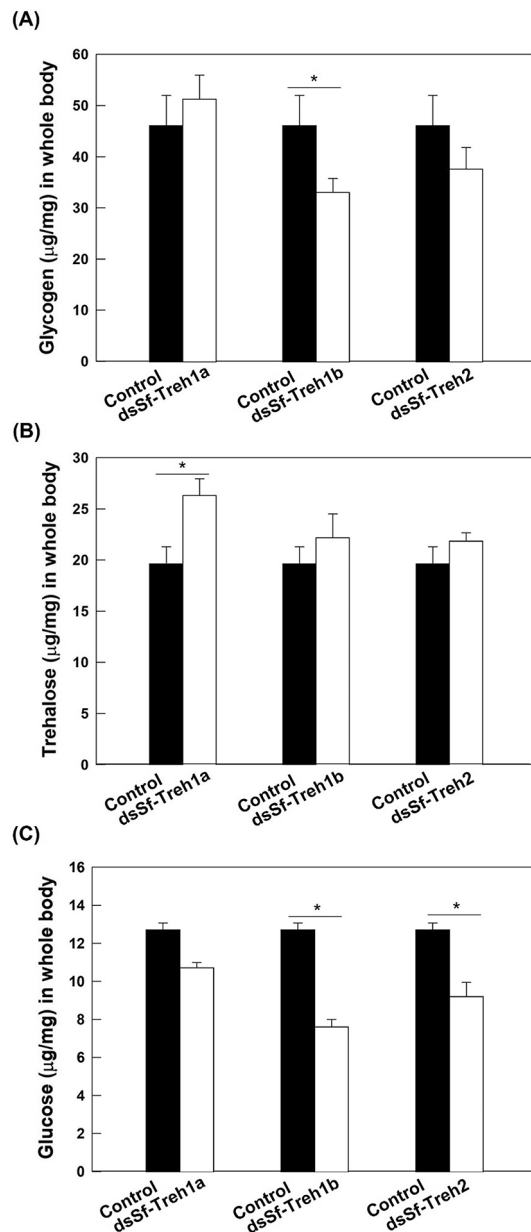


Fig. 4. Effect of dsTreh on trehalose (TRE), glycogen (GLY), and glucose (GLU) concentrations in the whole body of *S. frugiperda* larvae following rapid cold hardening (RCH). The whole-body concentrations of GLY (A), TRE (B), and GLU (C) in fifth instar larvae were measured 48 h after dsRNA injection, following RCH treatment. Each treatment was replicated three times with 10 individuals per replicate. Statistically significant differences between treatment groups and the control group (dsEGFP) are indicated by asterisks (* $p < 0.05$, ** $p < 0.01$, *** $p < 0.001$), as determined by one-way ANOVA followed by Tukey's post-hoc test.

showed a decreased level of GLU compared to the dsEGFP-treated larvae after exposure to RCH. In contrast, metabolomics has demonstrated the accumulation of other metabolites, polyols, and the build-up of GLU during RCH⁴⁹. RCH-induced GLU accumulation has been observed in similar studies in *Drosophila melanogaster*, indicating that the fast transport of GLU may be a standard feature during RCH. Although the GLU content in the hemolymph of a few individual larvae was barely detectable by HPLC in the dsSf-Treh2 treated group, in other insects and environments, the detection level was below the detection threshold in other insects and environments⁵⁰. We also observed a significant elevation of TRE in dsSf-Treh1a treated larvae than in dsSf-Treh1b and dsSf-Treh2. Evidence shows that TRE affects cold acclimatization and temperature regulation in *D. melanogaster*^{23,51}. This RNAi investigation in the FAW TRE pathway increased the TRE content to comparatively high levels after RCH treatment, indicating that Treh is involved in GLU generation during cold conditions and that inhibiting Treh leads to GLU energy minimization. These phenomena indicate insect metabolism during cold conditions or below freezing, which differs from insects under normal conditions.

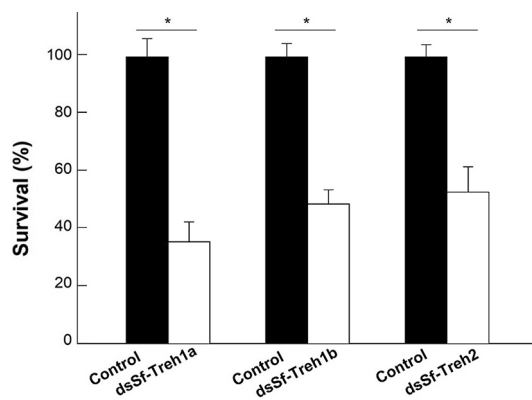


Fig. 5. Survival rates of FAW larvae following suppression of Treh dsRNAs and rapid cold hardening (RCH). After 48 h of successful suppression of the three Treh dsRNAs (dsSf-Treh1a, dsSf-Treh1b, and dsSf-Treh2), larvae were subjected to RCH, and survival rates were measured. A significant decrease in survival was observed in all dsSf-Treh-treated groups compared to the dsEGFP control group ($F(3,8) = 31.94, p < 0.001$). Post-hoc analyses (Tukey's test) confirmed statistically significant differences between each dsSf-Treh-treated group and the control ($*p < 0.05$). Assumption checks using Levene's test indicated that the variances were equal across groups ($p = 0.184$).

It is believed that in addition to the direct release of GLU into the circulating hemolymph, GLY in the fat body is converted to TRE⁵². We found that the dsEGFP-treated and post-RCH larvae could adapt to stress related to GLY, TRE, and GLU regulation. Therefore, reductions in GLU may have been caused by TRE and GLY competition. The levels of GLY and TRE were increased in the dsSf-Treh1a treated group, but Sf-Treh1b and Sf-Treh2 showed increased TRE but decreased GLY. Our results strongly support the view that reductions and elevations in TRE, GLY, and GLU in the dsSf-Treh1a treated group do not coincide with the dsSf-Treh1b and dsSf-Treh2 groups. In addition, neither TRE nor GLY could build during cold stress, and other carbohydrates could not be converted into TRE. These results are supported by prior findings that low-temperature changes significantly affect GLY, GLU, and TRE^{53,54}. A possible reason could be that GLY stores are restored through the hexokinase and trehalose-6-phosphate synthase/phosphatase pathway by converting GLU into GLY⁵⁵. The compensating zig saw effect observed in dsSf-Trehs treated groups needs further exploration to understand Treh's roles during RCH.

Many studies have proven that fat body TRE, GLU, myo-inositol, and other molecules are at elevated levels at the lowest temperatures^{56–58}. Adjustment between cryoprotectants, metabolites, and carbohydrates contributes to survival at cold temperatures. We investigated the survival of dsSf-Treh1a, 1b, and 2 injected FAW larvae after RCH treatment. The results show that FAW survives in cold environments through independent and shared mechanisms with TRE, GLU, and GLY. A knock-down of the *Sf-Treh1a*, *Sf-Treh1b*, and *Sf-Treh2* genes reduce their transcription levels, resulting in reduced survival and reduced ability to tolerate low temperatures. The most likely explanation for our findings is that these genes are required for cold tolerance in overwintering larvae.

Materials and methods

Insect rearing, exposure temperatures, and sample preparation

Fourth and fifth generations (F4 and F5) of FAW larvae used in this study were obtained from Frontier Agriculture Sciences (Newark, DE, USA). Laboratory conditions were maintained at a constant temperature of 26 °C, 70% relative humidity (RH), with a 14:10 h light cycle. Throughout their developmental stages (L1–L6), larvae were fed an artificial diet (Frontier Agriculture Sciences, Newark, DE, USA)⁵⁹. Early instar larvae were reared in aerated polypropylene containers (40 × 20 × 20 cm) from the time eggs were laid by adults. Once these larvae hatched and developed to the third instar stage, they were transferred to individual 8.5 cm diameter Petri dishes to prevent cannibalism.

Bioinformatics to predict *Treh1a*, *Treh1b*, and *Treh2* genes

The three Treh mRNA sequences were obtained from our previous whole FAW transcriptome analysis. The MegAlign - Clustal W software aligned the predicted amino acid sequences (DNASTAR Version 7.0). Using the MEGA 11.0 program (www.megasoftware.net), the phylogenetic trees were built using the neighbor-joining approach and the Poisson correction model (1,000 bootstrap repetitions to support branching clusters). The NCBI conserved domain database (www.ncbi.nlm.nih.gov/cdd) was used to predict the conserved domains of Treh genes. Protein motif analysis and the creation of 3D structures were done using UCSF Chimera (<https://www.cgl.ucsf.edu/chimera/>).

RNA extraction and RT-qPCR

Using Trizol reagent, RNA samples from FAW larvae were extracted by following the manufacturer's protocol (Invitrogen, Carlsbad, CA, USA). After extraction, RNA was resuspended in nuclease-free water and its

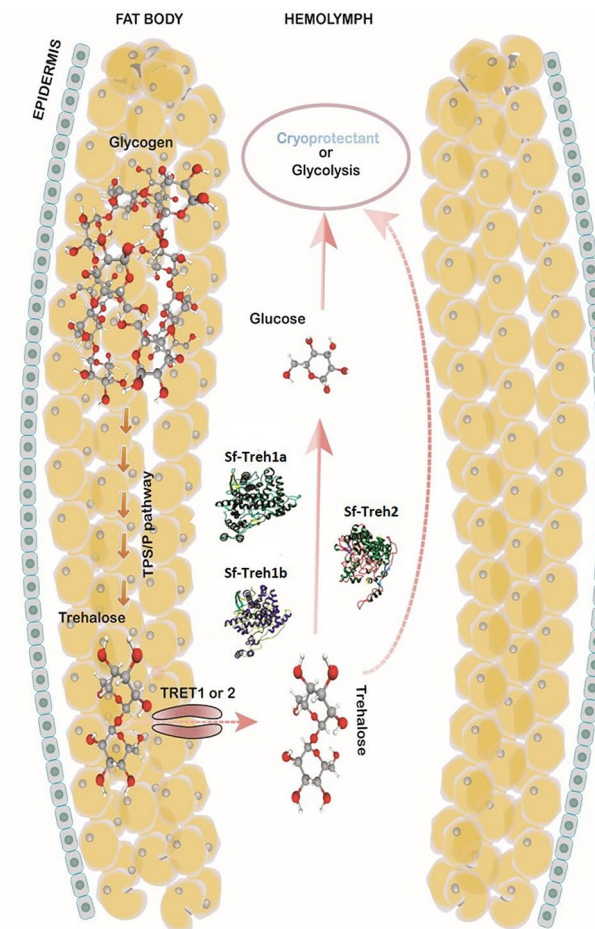


Fig. 6. Trehalose metabolism in *S. frugiperda*. Trehalose production, transport, and function are summarized, with red and white gradient arrows indicating the trehalose conversion from glycogen via the TPS/P pathway. The converted trehalose is transported via TRET 1 or 2 from the fat body to hemolymph. The glucose is produced by trehalose hydrolysis by trehalase enzymes. The protein 3D structures depict the three forms of *S. frugiperda* trehalase proteins. The dotted arrow represents the function of trehalose as a cryoprotectant, and the glucose act as a cryoprotectant or enters the glycolysis pathway. TPS/P, trehalose-6-phosphate synthase/phosphatase; TRET-1, trehalose-specific transporter, Sf-Treh1a, Sf-Treh1b, and Sf-Treh2 denotes *S. frugiperda* trehalase1a, 1b, and 2 respectively.

concentration was measured with a spectrophotometer (NanoDrop, Thermo Scientific, Wilmington, DE, USA). One microgram of RNA was used to synthesize the cDNA using RT Premix (Intron Biotechnology, Korea), as directed by the manufacturer. Following the manufacturer's instructions, all quantitative PCRs (qPCRs) in this study were performed on a Real-Time PCR apparatus (CFX Connect Real-Time PCR Detection System, Bio-Rad, Hercules, CA, USA). First, 1 μ L of cDNA template (100 ng), 1 μ L of each forward and reverse primer (Table S1), 10 μ L with IQ SYBR Green Super mix (Bio-Rad, Hercules, CA, USA), and finally, 7 μ L of nuclease-free water were added to the reaction mixture (20 μ L). The first 10 min of RT-qPCR cycling consisted of a 95 $^{\circ}$ C heat treatment, then denaturation at 94 $^{\circ}$ C for the 30s with 40 cycles, 30s at 55 $^{\circ}$ C for annealing, and 20 s at 72 $^{\circ}$ C for the extension. To normalize the gene expression levels in various treatments, the expression level of the reference gene EF1 was employed⁶⁰. The comparative CT ($2^{-\Delta\Delta CT}$) quantitative analysis was conducted⁶¹.

Rapid cold hardening bioassay

The RCH was measured in the L5 stage by exposure to 5 $^{\circ}$ C for 6 h before being subjected to -10 $^{\circ}$ C for an hour¹⁷. Test larvae individuals were arranged in a petri dish (10 mm \times 15 mm) for each treatment group. The survival rates were calculated after 1 h of recovery at 25 $^{\circ}$ C following cold treatment. Autonomous movement of individuals was required to be classified as living after mild stick probing on the abdomen.

Down-regulation of associated *trehalase* genes by RNA interference

RNAi was carried out with double-stranded RNA (dsRNA) synthesized using Megascript RNAi Kit (Ambion, Austin, TX, USA), following the instructions from the manufacturer and a previous method⁶². Gene-specific primers with T7 promoter sequence at their 5' ends were used to amplify partial segments (Table S1). The dsRNAs (dsSf-Treh1a, dsSf-Treh1b, and dsSf-Treh2) were synthesized at 37 $^{\circ}$ C for 4 h, and T7 RNA polymerase

was inactivated at 70 °C for 5 min. As control dsRNA, a 300 bp fragment of enhanced green fluorescent protein (dsEGFP) was synthesized. Each fifth instar larva was injected with three µg of dsRNA (1 µg/µL) by Nanolitre 2020 Injector equipped with SMART touch controller (World precision instruments, Sarasota, FL, USA). RNAi efficiency was determined by qPCR at 0, 12, 24, 36, 48, 72, 96, and 120 h post-injection. The treatment replicated three times with a minimum of 10 larvae were used.

Sample preparation and HPLC condition

Sample preparation for TRE and GLU, and HPLC quantification followed based on an earlier study with few modifications⁶³. Hemolymph of 10 fifth instar larvae (Day 1) was collected from each treatment and boiled with ethanol (1:8) in the heating block for 15 min, and then ethanol was evaporated at room temperature completely. The sample was centrifuged at 15,000 rpm for 5 min at 4 °C. The supernatant was eluted through a C18 silica cartridge (SepPak, Waters, Milford, MA, USA) with 80% ethanol. The filtrate was evaporated completely and dissolved in 100 µl HPLC-grade water. The final samples were filtered out by 0.22 µm syringe filters and directly used for HPLC in the Metabolomics Research Center for Functional Materials, Kyungshung University (Busan, Korea). A reversed-phase HPLC connected to ELSD (Shimadzu, Kyoto, Japan) was optimized to determine TRE and GLU simultaneously. HPLC separation was obtained using a Unison UK-Amino (250 × 4.6 mm) column. The mobile phase was made of water and acetonitrile. The ideal flow rate of 0.5 mL/min in isocratic elution conditions with a proportion of acetonitrile 70% over 10 min was used to optimize the separation of TRE and GLU. The ELSD detector temperature was set at 30 °C, and the column oven temperature was set at 40 °C. Calibration curves were generated in SigmaPlot by plotting the area against GLU and TRE concentrations. The areas of each standard were averaged and plotted against their known concentrations.

Glycogen, trehalase, and glucose colorimetric assay

The GLY, GLU (Abcam, Cambridge, MA, USA), and TRE assay kits (Megazyme, Bary, Ireland) were used to quantify the GLY, GLU, and TRE, respectively. Briefly, the dsRNAs-treated larvae were rinsed several times in cold phosphate buffer saline (1X) to remove the external debris attached to their body. Next, the dried and weighed larvae were homogenized manually in a glass homogenizer with recommended buffer solutions under cold conditions. Finally, the homogenate samples were centrifuged at 3,000 RPM for 5 min at 4 °C.

At this time required amount of supernatant was stored for protein assay. The supernatant liquid was transferred to new tubes and then heated at 75 °C for 10 min to solubilize proteins. After heating, the samples were centrifuged at the highest RPM for 5 min at 4 °C (Eppendorf, Hamburg, Germany). The clear supernatant was stored at -80 °C until the assay usage. A dilution series and comparison to single point standards for all compounds were used to estimate the concentration required for optimal measurement of the whole body's GLY, GLU, and TRE levels. Following the manufacturer's protocol, the protein was measured using the BCA kit (Gendepot, Barker, TX, USA) and the values were normalized. All experiments were performed in duplicates in a 96-well microtiter plate, and each assay's absorbance was read using a microtiter plate reader (Bio-Tek instruments, Bad Friedrichshall, Germany).

Data analysis

A total of three distinct biological replicates were used for each study. Before conducting ANOVA, preliminary assessments were performed to verify the assumptions of normality and homogeneity of variances. Normality was assessed using the Shapiro-Wilk test, and homogeneity of variances was tested with Levene's test. For the expression profile of trehalose biosynthesis genes in *S. frugiperda* tissues, a one-way ANOVA was conducted followed by Tukey's HSD test for post-hoc pairwise comparisons. For the developmental stage expression profile, either one-way or two-way ANOVA, followed by Tukey's HSD test, was applied based on the experimental design. One-way ANOVA with Tukey's post-hoc test was also used to analyze trehalose, glycogen, and glucose concentrations in whole-body samples following rapid cold hardening and survival reduction experiments. To assess the effects of dsRNA injections on the mRNA expression patterns of *Sf-Treh1a*, *Sf-Treh1b*, and *Sf-Treh2* across different time points, a series of statistical tests were conducted. First, the normality of the data was evaluated using the Shapiro-Wilk test (< 0.05). Homogeneity of variance across groups was assessed using Levene's test ($p > 0.05$). A Kruskal-Wallis test was used to compare gene expression levels across different time points. Post-hoc pairwise comparisons were performed using Dunn's test with Bonferroni correction. Significant pairwise differences were identified by Dunn's test and are represented by distinct significance letters in the corresponding bar plots (Tables 1, 2).

The R program (version 4.3.1)⁶⁴ and PROC GLM tool of the SAS software (SAS, Cary, NC, USA) was used for statistical analysis. The R program and Sigma Plot 14.0 software (SPSS Inc., Chicago, IL, USA) was used to visualize the results.

Conclusions

Among all three Treh genes, it was noted that the *Sf-Treh1a* gene is important for TRE production during RCH and GLU conversion. Although *Sf-Treh1b* and *Sf-Treh2* genes were involved in TRE hydrolysis, the GLU content was almost similar, but the TRE remained increased. Few studies have observed the roles of GLU, GLY, and TRE in RCH. FAW lacks a diapause mechanism; therefore, it cannot overwinter in cold climates but does so in selected geographical areas in their early stages^{65,66}. This study investigated three forms of Treh connected to the energy usage pathway essential for FAW survival under all climate conditions.

Based on these findings, trehalose acts as a cryoprotectant, whereas glucose contributes to the survival of whole animals exposed to freeze. This study found that FAW is not well accustomed to cold conditions in terms of glucose concentration levels. Because of this, other molecules may be used in combination with glucose and trehalose to provide a more comprehensive level of freeze tolerance protection and survivability. Additionally,

RNAi treatment group	Hemolymph from <i>S. frugiperda</i> 5 th instar larvae	
	Trehalose (mM/mL)	Glucose (mM/mL)
Control (dsEGFP)	5.26 ± 0.89 ^{e*}	3.21 ± 0.25 ^a
dsSf-Treh1a	11.26 ± 1.26 ^a	1.18 ± 0.12 ^c
dsSf-Treh1b	8.21 ± 0.85 ^b	2.48 ± 0.22 ^b
dsSf-Treh2	7.95 ± 0.91 ^b	2.14 ± 0.35 ^b

Table 1. Concentrations of trehalose and glucose in *S. frugiperda* hemolymph by HPLC. Values represent mean ± SEM ($n = 10$). Statistically significant differences between treatment groups are indicated by different superscript letters (one-way ANOVA with Tukey's post-hoc test, $p < 0.05$).

RNAi treatment group	Whole body from <i>S. frugiperda</i> 5 th instar larvae		
	Glycogen (µg/mg)	Trehalose (µg/mg)	Glucose (µg/mg)
Control (dsEGFP)	46.12 ± 5.85 ^{d*}	19.72 ± 1.58 ^c	12.71 ± 0.36 ^a
dsSf-Treh1a	51.25 ± 4.68 ^a	26.37 ± 2.25 ^a	7.61 ± 0.39 ^c
dsSf-Treh1b	33.05 ± 2.69 ^c	22.25 ± 1.58 ^b	10.72 ± 0.26 ^b
dsSf-Treh2	37.60 ± 6.00 ^b	21.91 ± 0.74 ^b	9.20 ± 0.74 ^b

Table 2. Concentrations of glycogen, trehalose, and glucose in *S. Frugiperda* whole body. Values represent mean ± SEM ($n = 10$). Statistically significant differences between treatment groups are indicated by different superscript letters (one-way ANOVA with Tukey's post-hoc test, $p < 0.05$).

further research is required to determine what glucose concentration is optimal for fall armyworms to tolerate cold temperatures and survive. As a result of exposure to cold, insects undergo a series of biochemical events that primarily involve cryoprotection and changes in energy metabolism^{67–69}. Possible future climate change and FAW outbreaks could make FAW one of agriculture's most destructive pests as it seeks to preserve its physiological energy equilibrium. However, more study models are recommended to support greater congruence with our results.

Data availability

The datasets generated during the current study are available in the Gene Expression Omnibus (GEO) database (<https://www.ncbi.nlm.nih.gov/geo/>, accession number GSE175545) and the Sequence Read Archive (SRA) (<https://www.ncbi.nlm.nih.gov/sra>, accession number SRP321312).

Received: 28 August 2023; Accepted: 6 November 2024

Published online: 09 November 2024

References

- Sparks, A. N. Fall armyworm (Lepidoptera: Noctuidae): Potential for area-wide management. *Fla. Entomol.* **69**, 603–614 (1986).
- Cruz, I., Figueiredo, M., Oliveira, A. C. & Vasconcelos, C. A. Damage of *Spodoptera frugiperda* (Smith) in different maize genotypes cultivated in soil under three levels of aluminum saturation. *Int. J. Pest Manage.* **45**, 293–296 (1999).
- Wu, M. F. et al. Overseas immigration of fall armyworm, *Spodoptera frugiperda* (Lepidoptera: Noctuidae), invading Korea and Japan in 2019. *Insect Sci.* **29**, 505–520 (2022).
- Guo, J., Zhao, J., He, K., Zhang, F. & Wang, Z. Potential invasion of the crop-devastating insect pest fall armyworm *Spodoptera frugiperda* to China. *Plant. Pro* **44**, 1–10 (2018).
- Du Plessis, H., Schlemmer, M. L. & Van den Berg, J. The effect of temperature on the development of *Spodoptera frugiperda* (Lepidoptera: Noctuidae). *Insects* **11**, 228 (2020).
- Dixon, A. F. & Hopkins, G. W. *Aphid Biodiversity under Environmental Change* (Springer, 2010).
- Birch, L. Experimental background to the study of the distribution and abundance of insects: I. The influence of temperature, moisture and food on the innate capacity for increase of three grain beetles. *Ecology* **34**, 698–711 (1953).
- Saikkonen, K. et al. Climate change-driven species' range shifts filtered by photoperiodism. *Nat. Clim. Change* **2**, 239–242 (2012).
- Faaborg, J. *Saving Migrant Birds* (University of Texas, 2021).
- Salt, R. W. Cold-hardiness of insects. In *Proc. 10th Int. Congr Ent.*, Vol. 2 73–77 (1958).
- Song, Y. et al. Physiological characteristics and cold tolerance of overwintering eggs in *Gomphoceris Sibiricus* L. (Orthoptera: Acrididae). *Arch. Insect Biochem.* **108**, e21846 (2021).
- Feng, Y., Zhang, L., Li, W., Yang, X. & Zong, S. Cold hardiness of overwintering larvae of Sphenoptera sp. (Coleoptera: Buprestidae) in Western China. *J. Econ. Entomol.* **111**, 247–251 (2018).
- Toxopeus, J. & Sinclair, B. J. Mechanisms underlying insect freeze tolerance. *Biol. Rev.* **93**, 1891–1914 (2018).
- Lee, R. E. Jr, Chen, C. & Denlinger, D. L. A rapid cold-hardening process in insects. *Science* **238**, 1415–1417 (1987).
- Storey, K. B. & Storey, J. M. *Insects at Low Temperature* (Springer US, 1991).
- Vatanparast, M. & Park, Y. Cold tolerance strategies of the fall armyworm, *Spodoptera frugiperda* (Smith) (Lepidoptera: Noctuidae). *Sci. Rep.* **12**, 1–16 (2022).
- Park, Y. & Kim, Y. RNA interference of glycerol biosynthesis suppresses rapid cold hardening of the beet armyworm, *Spodoptera exigua*. *J. Exp. Biol.* **216**, 4196–4203 (2013).

18. Xu, H. J. et al. Two insulin receptors determine alternative wing morphs in planthoppers. *Nature* **519**, 464–467 (2015).
19. Feng, Y. et al. Seasonal changes in supercooling capacity and major cryoprotectants of overwintering a sian longhorned beetle (*Anoplophora glabripennis*) larvae. *Agr. Entomol.* **18**, 302–312 (2016).
20. Košťál, V., Zahradníčková, H., Šimek, P. & Zelený, J. Multiple component system of sugars and polyols in the overwintering spruce bark beetle, *Ips typographus*. *J. Insect Physiol.* **53**, 580–586 (2007).
21. Hou, M., Lin, W. & Han, Y. Seasonal changes in supercooling points and glycerol content in overwintering larvae of the Asiatic rice borer from rice and water-oat plants. *Environ. Entomol.* **38**, 1182–1188 (2009).
22. Saeidi, F., Mikani, A. & Moharramipour, S. Thermal tolerance variations and physiological adjustments in a winter active and a summer active aphid species. *J. Therm. Biol.* **98**, 102950 (2021).
23. Overgaard, J. et al. Metabolomic profiling of rapid cold hardening and cold shock in *Drosophila melanogaster*. *J. Insect Physiol.* **53**, 1218–1232 (2007).
24. Yamada, T., Habara, O., Kubo, H. & Nishimura, T. Fat body glycogen serves as a metabolic safeguard for the maintenance of sugar levels in *Drosophila*. *Development* **145**, dev165910 (2018).
25. Worland, M. R., Grubor-Lajsic, G. & Montiel, P. O. Partial desiccation induced by sub-zero temperatures as a component of the survival strategy of the Arctic collembolan *Onychiurus arcticus* (Tullberg). *J. Insect Physiol.* **44**, 211–219 (1998).
26. Tang, B. et al. Invertebrate trehalose-6-phosphate synthase gene: Genetic architecture, biochemistry, physiological function, and potential applications. *Front. Physiol.* **9**, 30 (2018).
27. Liu, X. et al. Knockdown of the trehalose-6-phosphate synthase gene using RNA interference inhibits synthesis of trehalose and increases lethality rate in Asian citrus psyllid, *Diaphorina citri* (Hemiptera: Psyllidae). *Insects* **11**, 605 (2020).
28. Tang, B. et al. Characterization and expression patterns of a membrane-bound trehalase from *Spodoptera exigua*. *BMC Mol. Biol.* **9**, 51 (2008).
29. Arrese, E. L. & Soulages, J. L. Insect fat body: Energy, metabolism, and regulation. *Annu. Rev. Entomol.* **55**, 207–225 (2010).
30. Skowronek, P., Wójcik, L. & Strachecka, A. Fat body-multifunctional insect tissue. *Insects* **12**, 547 (2021).
31. Andreadis, S. S. & Athanassiou, C. G. A review of insect cold hardiness and its potential in stored product insect control. *Crop Prot.* **91**, 93–99 (2017).
32. Salt, R. W. Principles of insect cold-hardiness. *Annu. Rev. Entomol.* **6**, 55–74 (1961).
33. Shi, Z. K. et al. Effects of starvation on the carbohydrate metabolism in *Harmonia axyridis* (Pallas). *Biol. Open.* **6**, 1096–1103 (2017).
34. Tang, B., Xu, Q., Zhao, L., Wang, S. & Zhang, F. Progress in research on the characteristics and functions of trehalose and the TPS gene in insects. *Chin. J. Entomol.* **51**, 1397–1405 (2014).
35. Zeng, B. et al. Effect of long-term cold storage on trehalose metabolism of pre-wintering *Harmonia axyridis* adults and changes in morphological diversity before and after wintering. *PLoS One* **15**, e0230435 (2020).
36. Yasugi, T., Yamada, T. & Nishimura, T. Adaptation to dietary conditions by trehalose metabolism in *Drosophila*. *Sci. Rep.* **7**, 1619 (2017).
37. Teets, N. M. & Denlinger, D. L. Physiological mechanisms of seasonal and rapid cold-hardening in insects. *Physiol. Entomol.* **38**, 105–116 (2013).
38. Denlinger, D. L. & Lee, R. E. Jr *Low Temperature Biology of Insects* (Cambridge University Press, 2010).
39. Wang, G. et al. Trehalose and glucose levels regulate feeding behavior of the phloem-feeding insect, the pea aphid *Acyrtosiphon pisum* Harris. *Sci. Rep.* **11**, 15864 (2021).
40. Perez, R. & Aron, S. Protective role of trehalose in the Namib desert ant, *Ocymyrmex robustior*. *J. Exp. Biol.* **226**, jeb245149 (2023).
41. Shukla, E., Thorat, L. J., Nath, B. B. & Gaikwad, S. M. Insect trehalase: Physiological significance and potential applications. *Glycobiology* **25**, 357–367 (2014).
42. Lü, X., Han, S., Li, Z., Li, L. & Li, J. Gene characterization and enzymatic activities related to trehalose metabolism of *in vitro* reared *Trichogramma dendrolimi* Matsumura (Hymenoptera: Trichogrammatidae) under sustained cold stress. *Insects* **11**, 767 (2020).
43. Tang, B. et al. Knockdown of five trehalase genes using RNA interference regulates the gene expression of the chitin biosynthesis pathway in *Tribolium castaneum*. *BMC Biotech.* **16**, 67 (2016).
44. Kamei, Y., Hasegawa, Y., Niimi, T., Yamashita, O. & Yaginuma, T. Trehalase-2 protein contributes to trehalase activity enhanced by diapause hormone in developing ovaries of the silkworm, *Bombyx mori*. *J. Insect Physiol.* **57**, 608–613 (2011).
45. Su, Z. H. et al. Molecular characterization of ovary trehalase of the silkworm, *Bombyx mori* and its transcriptional activation by diapause hormone. *BBA* **1218**, 366–374 (1994).
46. Santos, R. et al. Gene identification and enzymatic properties of a membrane-bound trehalase from the ovary of *Rhodnius prolixus*. *Arch. Insect Biochem.* **81**, 199–213 (2012).
47. Ayriñac, A. et al. Cold adaptation in geographical populations of *Drosophila melanogaster*: Phenotypic plasticity is more important than genetic variability. *Func. Ecol.*, 700–706 (2004).
48. Lee, R. E. Jr & Denlinger, D. L. Cold tolerance in diapausing and non-diapausing stages of the flesh fly, *Sarcophaga crassipalpis*. *Physiol. Entomol.* **10**, 309–315 (1985).
49. Michaud, M. R. & Denlinger, D. L. Shifts in the carbohydrate, polyol, and amino acid pools during rapid cold hardening and diapause associated cold hardening in flesh flies (*Sarcophaga crassipalpis*): A metabolomic comparison. *J. Comp. Physiol. B* **177**, 753–763 (2007).
50. Sawczyn, T. et al. Alteration of carbohydrates metabolism and midgut glucose absorption in *Gromphadorhina portentosa* after subchronic exposure to imidacloprid and fenitrothion. *J. Environ. Sci. Health A* **47**, 1644–1651 (2012).
51. Košťál, V. et al. Long-term cold acclimation extends survival time at 0°C and modifies the metabolomic profiles of the larvae of the fruit fly *Drosophila melanogaster*. *PLoS One* **6**, e25025 (2011).
52. Chang, C. F. *Carbohydrates-Comprehensive Studies on Glycobiology and Glycotechnology* (InTechOpen, 2012).
53. Wan, S. et al. Regulatory role of trehalose metabolism in cold stress of *Harmonia axyridis* laboratory and overwinter populations. *Agronomy* **13**, 148 (2023).
54. Shi, Z. et al. Two novel soluble trehalase genes cloned from *Harmonia axyridis* and regulation of the enzyme in a rapid changing temperature. *Comp. Biochem. Physiol. B* **198**, 10–18 (2016).
55. Roach, P. J., Depaoli-Roach, A. A., Hurley, T. D. & Tagliabacci, V. S. Glycogen and its metabolism: Some new developments and old themes. *Biochem* **441**, 763–787 (2012).
56. Izadi, H., Mohammadzadeh, M. & Mehrabian, M. Changes in biochemical contents and survival rates of two stored product moths under different thermal regimes. *J. Therm. Biol.* **80**, 7–15 (2019).
57. Mohammadzadeh, M. & Izadi, H. Cold acclimation of *Trogoderma granarium* Everts is tightly linked to regulation of enzyme activity, energy content, and ion concentration. *Front. Physiol.* **9**, 1427 (2018).
58. Saeidi, F., Moharramipour, S. & Mikani, A. Effect of cold acclimation and rapid cold hardiness on cold tolerance and cryoprotectants of the greenbug *Schizaphis graminum* (Hemiptera: Aphididae). *JESI* **37**, 193–205 (2017).
59. Vatanparast, M., Ahmed, S., Sajjadian, S. M. & Kim, Y. A prophylactic role of a secretory PLA2 of *Spodoptera exigua* against entomopathogens. *Dev. Comp. Immunol.* **95**, 108–117 (2019).
60. Shu, B. et al. Identification of azadirachtin responsive genes in *Spodoptera frugiperda* larvae based on RNA-seq. *Pest. Biochem. Physiol.* **172**, 104745 (2021).
61. Livak, K. J. & Schmittgen, T. D. Analysis of relative gene expression data using real-time quantitative PCR and the 2^{-ΔΔCT} method. *Methods* **25**, 402–408 (2001).

62. Sajjadian, S. M., Vatanparast, M. & Kim, Y. Toll/IMD signal pathways mediate cellular immune responses via induction of intracellular PLA 2 expression. *Arch. Insect Biochem.* **101**, e21559 (2019).
63. Nakamatsu, Y. & Tanaka, T. Correlation between concentration of hemolymph nutrients and amount of fat body consumed in lightly and heavily parasitized hosts (*Pseudaletia Separata*). *J. Insect Physiol.* **50**, 135–141 (2004).
64. R Core Team. *R: A Language and Environment for Statistical Computing* (R Foundation for Statistical Computing, 2020).
65. Luginbill, P. *The Fall Armyworm* (US Department of Agriculture, 1928).
66. Johnson, S. Migration and the life history strategy of the fall armyworm, *Spodoptera frugiperda* in the western hemisphere. *Int. J. Trop. Insect Sci.* **8**, 543–549 (1987).
67. Poelchau, M. F., Reynolds, J. A., Elsik, C. G., Denlinger, D. L. & Armbruster, P. A. RNA-Seq reveals early distinctions and late convergence of gene expression between diapause and quiescence in the Asian tiger mosquito, *Aedes albopictus*. *J. Exp. Biol.* **216**, 4082–4090 (2013).
68. Ragland, G. J., Denlinger, D. L. & Hahn, D. A. Mechanisms of suspended animation are revealed by transcript profiling of diapause in the flesh fly. *Proc. Natl. Acad. Sci.* **107**, 14909–14914 (2010).
69. Williams, C. M. et al. Understanding evolutionary impacts of seasonality: An introduction to the symposium. *ICB* **57**, 921–933 (2017).

Acknowledgements

This research was supported by a research fund (PQ20201A011) of Animal and Plant Quarantine Agency, Korea and the National Research Foundation of Korea (NRF) grant funded by the Korea government (MSIT) (RS-2024-00357273) to Y.P.

Author contributions

Y.P. conceived the idea, designed the experiments; A.G. and Y.P. performed the experiments; A.G., H.M., and Y.P. analyzed the data; A.G. and Y.P. co-wrote the manuscript; A.G., H.M., and Y.P. discussed the results and commented on the manuscript.

Declarations

Competing interests

The authors declare no competing interests.

Additional information

Supplementary Information The online version contains supplementary material available at <https://doi.org/10.1038/s41598-024-79082-y>.

Correspondence and requests for materials should be addressed to Y.P.

Reprints and permissions information is available at www.nature.com/reprints.

Publisher's note Springer Nature remains neutral with regard to jurisdictional claims in published maps and institutional affiliations.

Open Access This article is licensed under a Creative Commons Attribution-NonCommercial-NoDerivatives 4.0 International License, which permits any non-commercial use, sharing, distribution and reproduction in any medium or format, as long as you give appropriate credit to the original author(s) and the source, provide a link to the Creative Commons licence, and indicate if you modified the licensed material. You do not have permission under this licence to share adapted material derived from this article or parts of it. The images or other third party material in this article are included in the article's Creative Commons licence, unless indicated otherwise in a credit line to the material. If material is not included in the article's Creative Commons licence and your intended use is not permitted by statutory regulation or exceeds the permitted use, you will need to obtain permission directly from the copyright holder. To view a copy of this licence, visit <http://creativecommons.org/licenses/by-nc-nd/4.0/>.

© The Author(s) 2024